Structural and Electronic Properties of MXene Flakes: From Edge Effects to Bandgap Evolution

*Miquel Allés,[a] Sergi Vela,[b] Ángel Morales-García,[a] Francesc Viñes,[a] Carmen Sousa[a,]**

[a] Departament de Ciència de Materials i Química Física & Institut de Química Teòrica i Computacional (IQTCUB), Universitat de Barcelona, c/Martí i Franquès 1-11, 08028 Barcelona, Spain
[b] Institut de Química Avançada de Catalunya (IQAC-CSIC), c/ Jordi Girona 18-26, 08028 Barcelona, Spain

* corresponding author e-mail: c.sousa@ub.edu

Table of contents

Table S1. Cleavage energies, $E_{Cleavage}$, of M_2C MXenes obtained from nanoribbons exposing each surface. Data is disclosed in two sections, separating ABC and ABA stacking for pristine MXenes. $(10\bar{1}0)$, $(11\bar{2}0)_{Non\text{-}polar}$, and $(11\bar{2}0)_{Polar}$ surfaces are shown for ABC stacking and $(10\bar{1}0)$ and $(11\bar{2}0)$ for ABA. All values are given in J/m^2.

ABC	**Sc_2C**	**Ti_2C**	**V_2C**	**Cr_2C**	**ABA**	**Cr_2C**
$(10\bar{1}0)$	7.30	9.77	14.00	16.76	**$(10\bar{1}0)$**	11.25
$(11\bar{2}0)_{Non\text{-}polar}$	6.56	8.70	11.08	8.96	**$(11\bar{2}0)$**	9.99
$(11\bar{2}0)_{Polar}$	8.76	11.83	16.02	20.77		
	Y_2C	**Zr_2C**	**Nb_2C**			**Mo_2C**
$(10\bar{1}0)$	5.78	8.91	12.23		**$(10\bar{1}0)$**	9.88
$(11\bar{2}0)_{Non\text{-}polar}$	5.38	7.94	9.45		**$(11\bar{2}0)$**	9.95
$(11\bar{2}0)_{Polar}$	6.83	10.26	13.65			
		Hf_2C	**Ta_2C**			**W_2C**
$(10\bar{1}0)$		9.77	14.34		**$(10\bar{1}0)$**	12.14
$(11\bar{2}0)_{Non\text{-}polar}$		8.43	10.29		**$(11\bar{2}0)$**	12.35
$(11\bar{2}0)_{Polar}$		11.21	15.33			

Table S2. Regression data of Figures 3 and S2 corresponding to differences in energy per stoichiometric unit between flakes and periodic slabs of M_2C/M_2CO_2 MXenes *vs.* number of stoichiometric units of flakes to the power of -1/2. Each MXene is referred to its own slab surface and data for Cr with ABA structure is in parenthesis and italics.

	Sc_2C	**Ti_2C**	**V_2C**	**Cr_2C**
Intercept	0.000	-0.007	-0.028	-0.051 (*0.036*)
Slope	5.561	6.692	7.107	6.489 (*7.657*)
R	0.999	0.999	0.999	0.999 (*0.967*)
	Y_2C	**Zr_2C**	**Nb_2C**	**Mo_2C**
Intercept	0.005	-0.012	-0.047	-0.053
Slope	4.922	7.121	7.720	8.888
R	0.999	0.999	0.999	0.999
		Hf_2C	**Ta_2C**	**W_2C**
Intercept	—	-0.020	-0.050	-0.028
Slope	—	7.465	8.727	10.905
R	—	0.999	0.999	0.995

	Sc_2CO_2	**Ti_2CO_2**	**V_2CO_2**	**Cr_2CO_2**
Intercept	-0.114	0.289	0.039	-0.059 (*0.182*)
Slope	7.401	10.284	7.668	4.287 (*10.506*)
R	0.998	0.996	0.999	0.978 (*0.998*)
	Y_2CO_2	**Zr_2CO_2**	**Nb_2CO_2**	**Mo_2CO_2**
Intercept	0.050	0.062	0.212	-0.154
Slope	5.585	13.256	9.443	13.348
R	0.988	0.999	0.997	0.994
		Hf_2CO_2	**Ta_2CO_2**	**W_2CO_2**
Intercept	—	-0.102	0.215	0.090
Slope	—	15.469	10.906	12.663
R	—	0.996	0.998	0.997

Table S3. M_2C and M_2CO_2 MXenes calculated parameters d(CC), $d(M_{top}M_{top})$, $d(M_{bot}M_{bot})$, $h(M_{top}M_{bot})$, and $h(O_{top}O_{bot})$ compared with periodic cell parameter a, and height h between metal (or oxygen for M_2CO_2 MXenes) layers of the periodic systems obtained by Ontiveros *et al*.[20] All data correspond to the biggest calculated flake and is shown in Å. For Cr, ABA structures are shown in parenthesis and italics.

M_2C	***d*(CC)**	***d*($M_{top}M_{top}$)**	***d*($M_{bot}M_{bot}$)**	**Slab *a***	***h*($M_{top}M_{bot}$)**	**Slab *h***
Sc_2C	3.293	3.287	3.287	3.328	2.441	2.409
Y_2C	3.527	3.533	3.533	3.588	2.700	2.661
Ti_2C	3.036	3.014	2.997	3.075	2.305	2.250
Zr_2C	3.267	3.244	3.244	3.274	2.542	2.544
Hf_2C	3.220	3.194	3.194	3.212	2.553	2.544
V_2C	2.906	2.862	2.863	2.900	2.165	2.174
Nb_2C	3.133	3.095	3.095	3.130	2.368	2.388
Ta_2C	3.099	3.059	3.059	3.084	2.428	2.436
Cr_2C	2.860 (*2.673*)	2.794 (*2.623*)	2.792 (*2.621*)	2.807 (*2.638*)	2.029 (*2.478*)	2.112 (*2.521*)
Mo_2C	2.852	2.836	2.840	2.850	2.621	2.742
W_2C	2.866	2.833	2.833	2.847	2.741	2.788

M_2CO_2	***d*(CC)**	***d*($M_{top}M_{top}$)**	***d*($M_{bot}M_{bot}$)**	**Slab *a***	***h*($O_{top}O_{bot}$)**	**Slab *h***
Sc_2CO_2	3.458	3.327	3.488	3.405	3.653	3.892
Y_2CO_2	3.721	3.614	3.789	3.702	3.653	4.067
Ti_2CO_2	3.058	3.045	3.046	3.011	4.449	4.467
Zr_2CO_2	3.316	3.322	3.322	3.303	4.628	4.697
Hf_2CO_2	3.278	3.300	3.291	3.372	4.533	4.379
V_2CO_2	2.919	2.913	2.913	2.875	4.476	4.456
Nb_2CO_2	3.143	3.140	3.141	3.132	4.666	4.722
Ta_2CO_2	3.131	3.134	3.134	3.113	4.681	4.700
Cr_2CO_2	2.859 *(2.771)*	2.850 *(2.658)*	2.852 *(2.659)*	2.860 *(2.650)*	4.494 *(4.872)*	4.477 *(4.933)*
Mo_2CO_2	2.865	2.867	2.872	2.870	5.123	5.274
W_2CO_2	2.895	2.877	2.876	2.879	5.070	5.297

Figure S1. Cleavage energy calculation workflow along the three main steps: 1) Optimisation of the orthorhombic *c*(1×1) cell. 2) Replication of the *c*(1×1) cell to obtain a *c*(3×3) supercell. 3) Addition of 10 Å vacuum to the *c*(3×3) supercell in the direction normal to the desired surface. The periodic unit cells are represented from a top view and indicated with black lines.

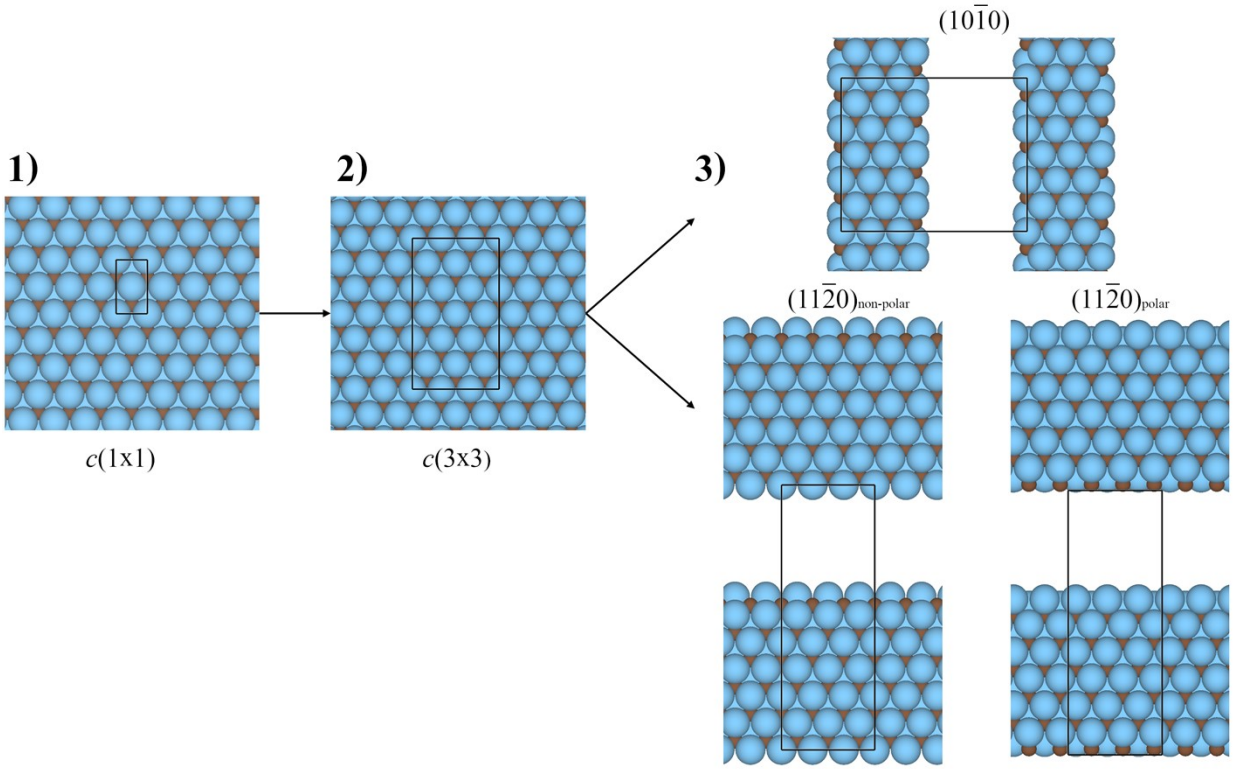

Figure S2. Differences in energy per stoichiometric unit between flakes and periodic slabs of M_2C (top) and M_2CO_2 (bottom) MXenes *vs.* number of stoichiometric units of flakes. Metals are differentiated by colors, and Stacking-Site is shown in solid lines and crosses for ABC-H_{MX}, solid lines and circles for ABC-H_M, and dotted lines and triangles for ABA-H_X. Each MXene is referred to its own slab surface.

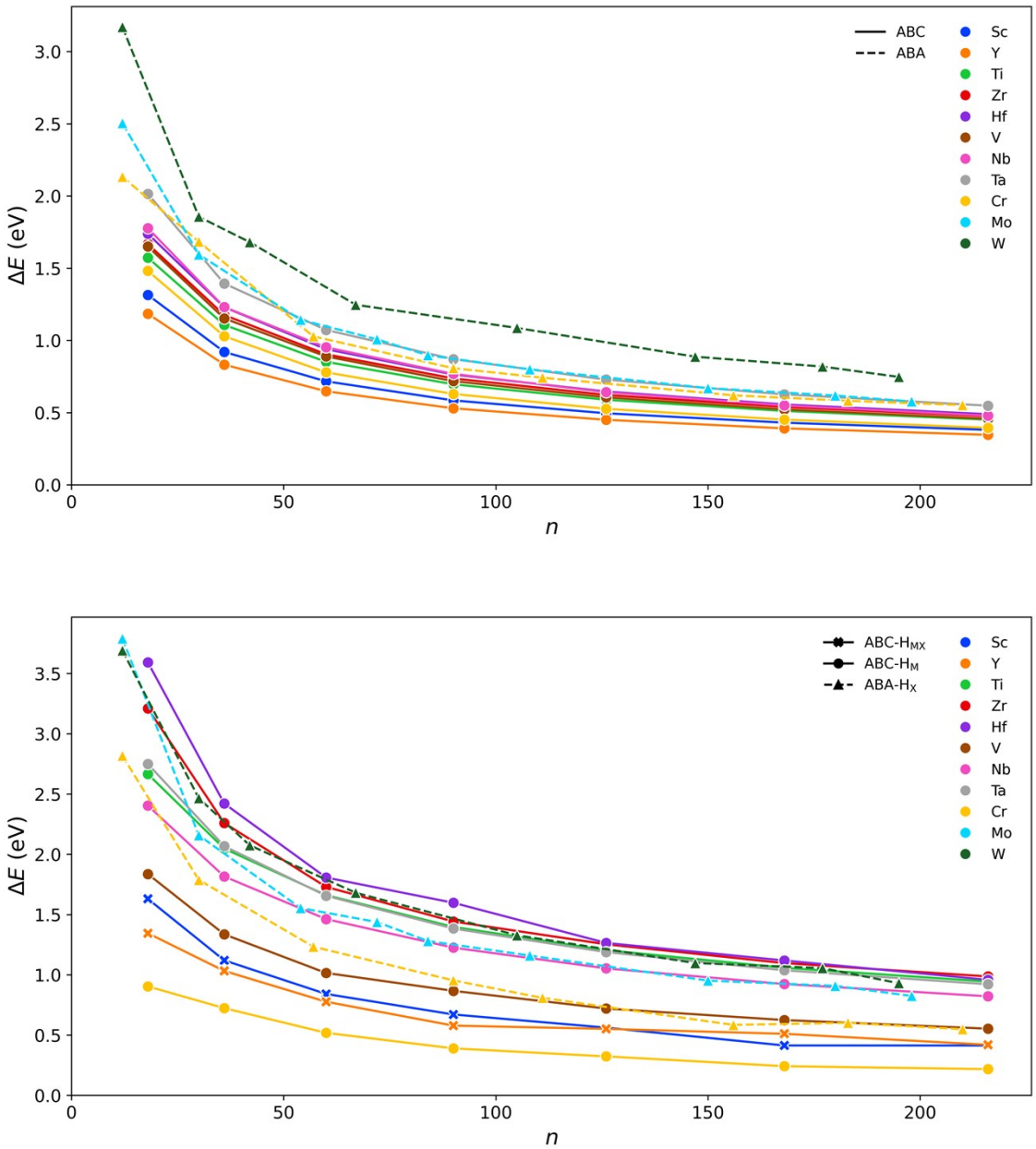

Figure S3. Differences in energy per stoichiometric unit between flakes and periodic slabs of M_2CO_2 MXenes *vs.* number of stoichiometric units of flakes to the power of -1/2. Metals are differentiated by colors, and Stacking-Site is shown in solid lines and crosses for ABC-H_{MX}, solid lines and circles for ABC-H_M, and dotted lines and triangles for ABA-H_X. Each MXene is referred to its own slab surface.

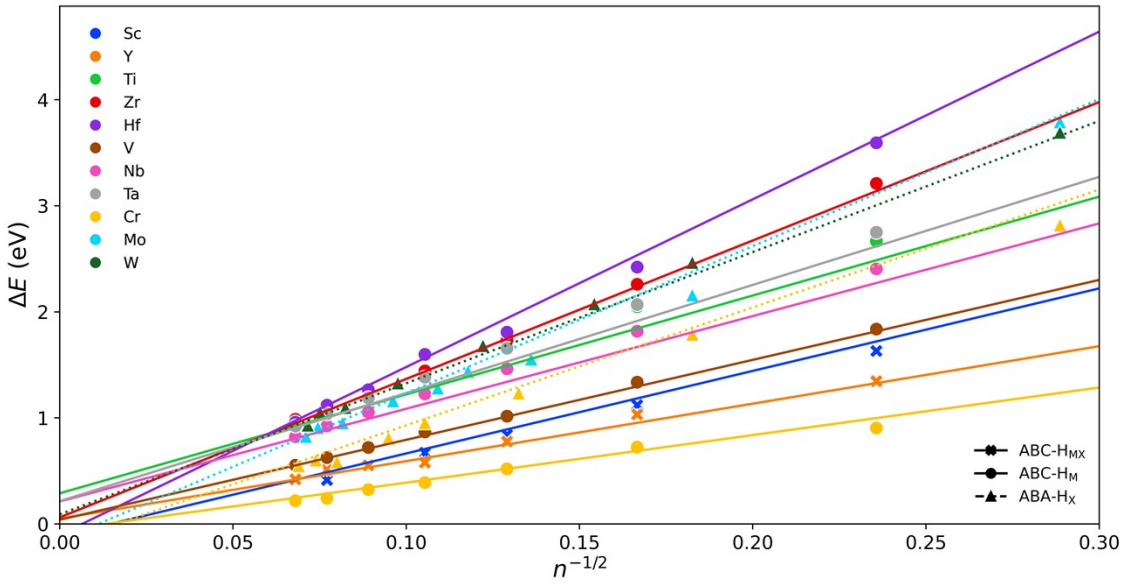

Figure S4. Evolution of d(CC), d($M_{top}M_{top}$), d($M_{bot}M_{bot}$), and h($M_{top}M_{bot}$) structural parameters on M_2C (top) and d(CC), d($M_{top}M_{top}$), d($M_{bot}M_{bot}$), and h($O_{top}O_{bot}$) on M_2CO_2 (bottom) MXenes for different flake sizes. All values are given in Å.

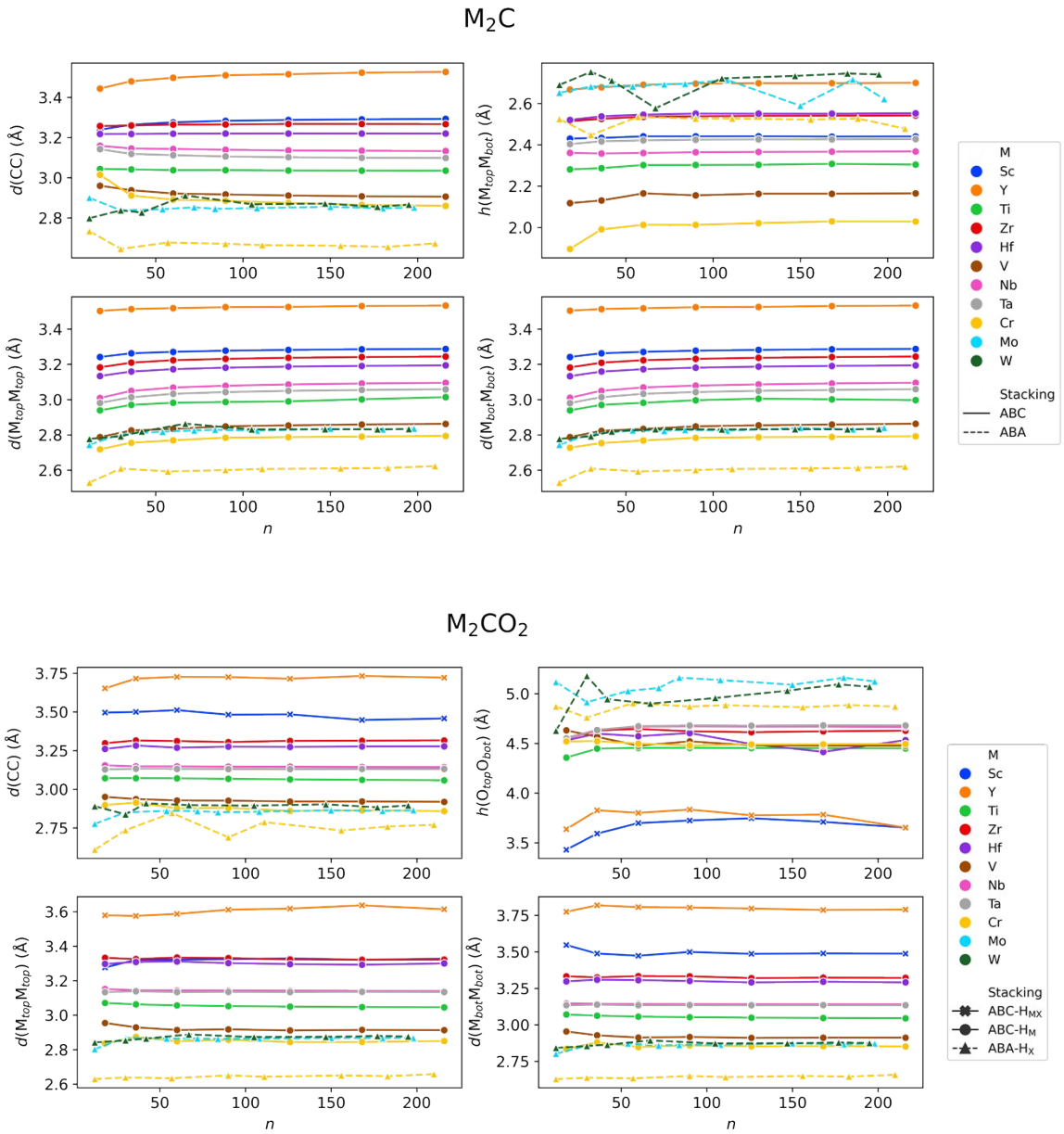

Figure S5. Evolution of the HOMO-LUMO gap, E_{HL}, for M_2C MXenes, calculated at PBE level.

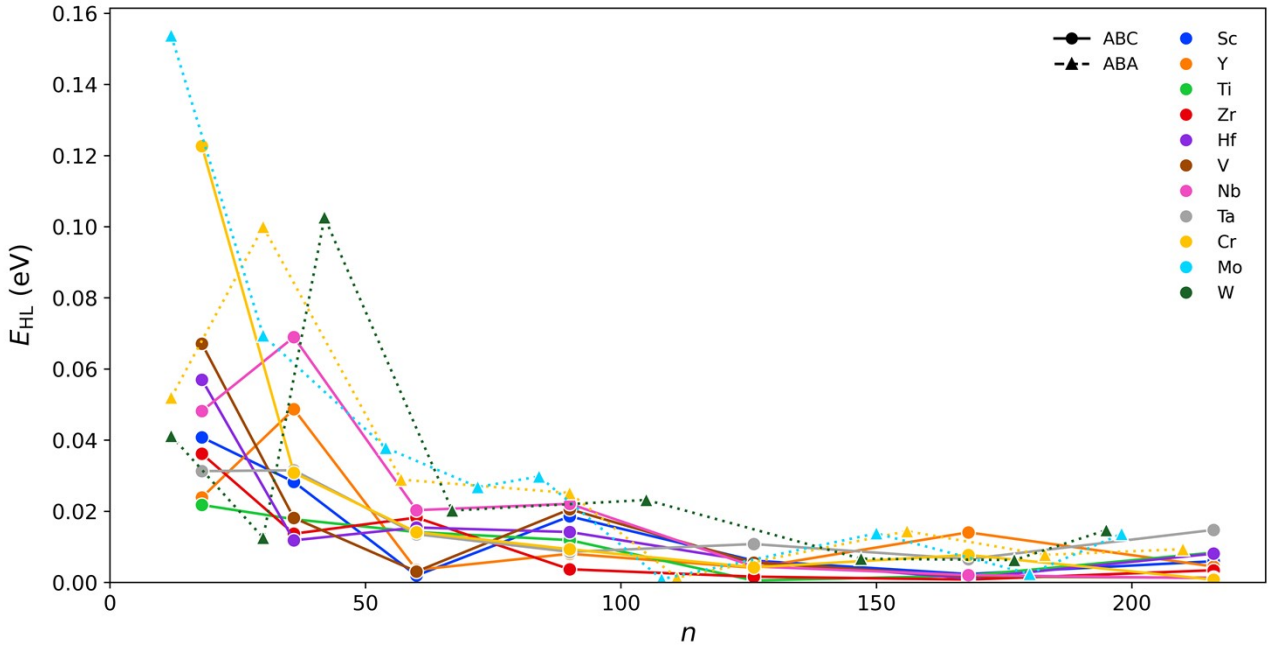

Figure S6. Evolution of the HOMO-LUMO gap, E_{HL}, for M_2CO_2 MXenes calculated at PBE level.

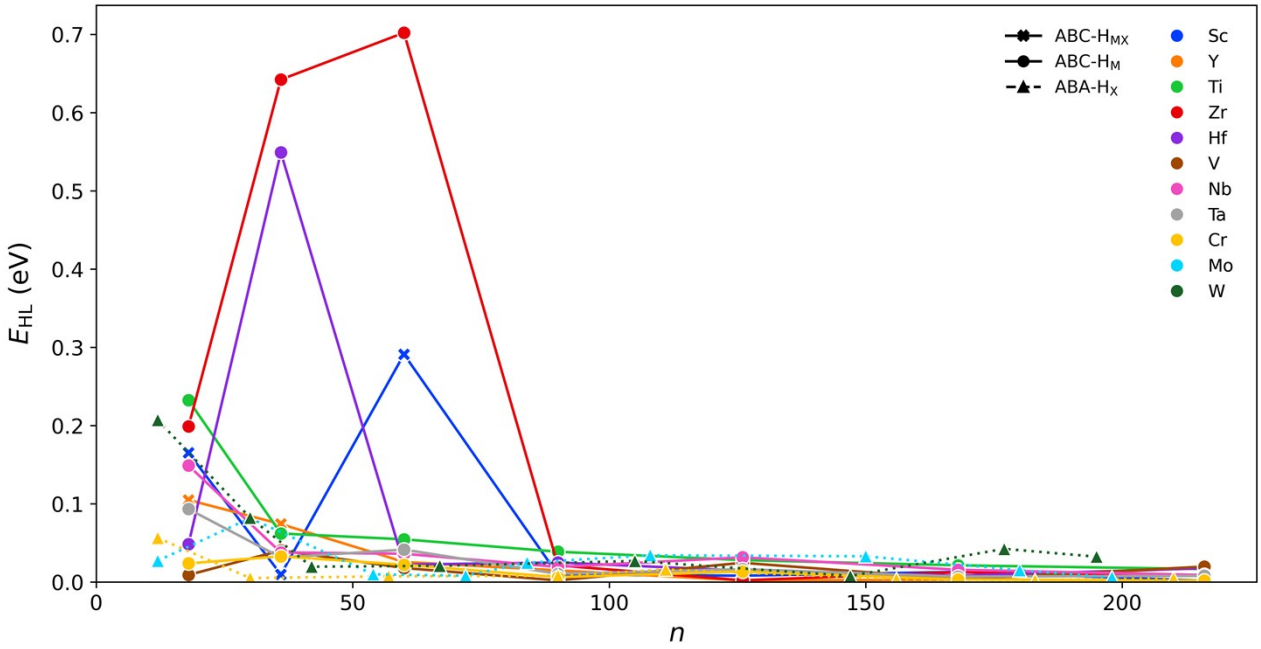

Figure S7. PBE0 total DOS of $(Ti_2CO_2)_{18}$, $(Ti_2CO_2)_{36}$, $(Ti_2CO_2)_{60}$, $(Ti_2CO_2)_{126}$, and $(Ti_2CO_2)_{216}$ flakes represented with 0.1 and 0.01 eV smearing in black and red lines, respectively. All densities within the displayed energy window have been normalized to 1. Fermi level has been set to 0 on the total DOS and it is shown in black.

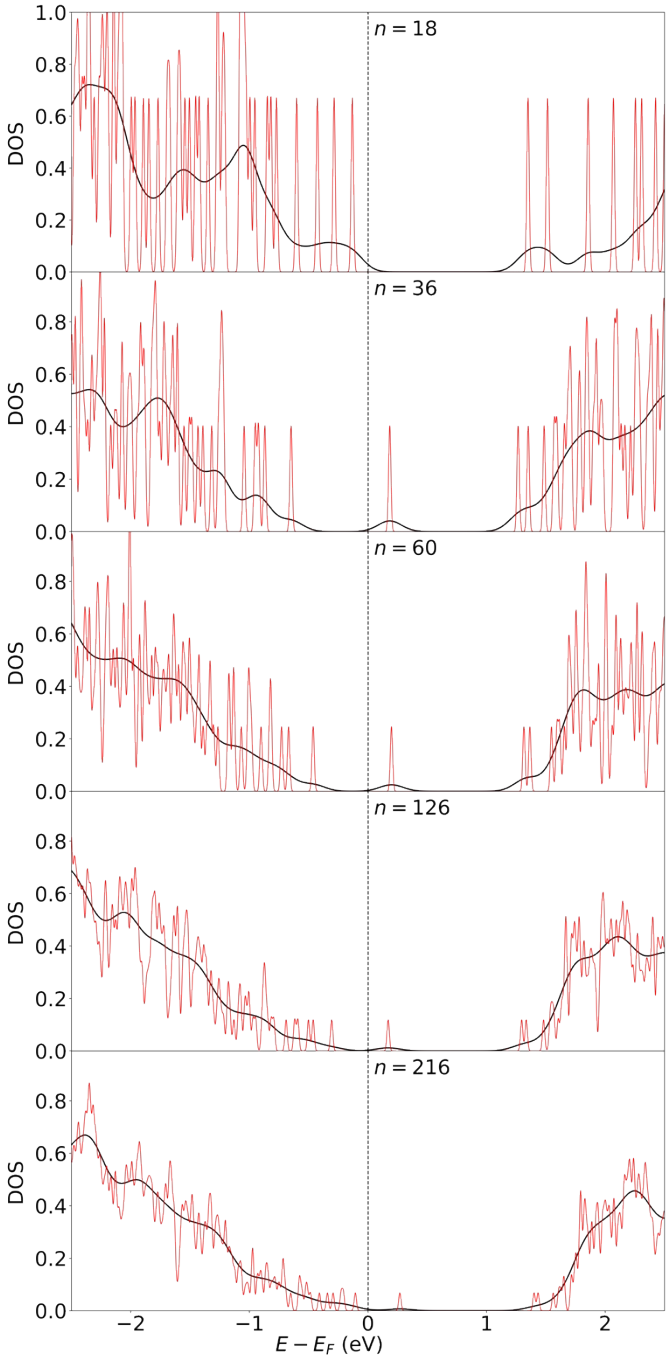

Figure S8. Corrected VBM and CBM energetic alignment for the largest Sc_2CO_2, Y_2CO_2, Ti_2CO_2, Zr_2CO_2 and Hf_2CO_2 flakes. VBM energy corresponds to the E_F^c energy of each flake while CBM refers to $E_F^c + E_g^c$ (see text). Hydrogen reduction, H^+/H_2, and water oxidation, H_2O/O_2, potentials are defined in dashed lines.